Electronic Supplementary Material (ESI) for Materials Horizons.
This journal is © The Royal Society of Chemistry 2018

Supporting Information for Crystalline silicon solar cells with tetracene interlayers: the path to silicon-singlet fission heterojunction devices

August 3, 2018

1 Ex-situ UPS study of Tc/c-Si interface

The secondary electron cut-off (SECO) and valence band/HOMO spectra are shown in Fig. 1.

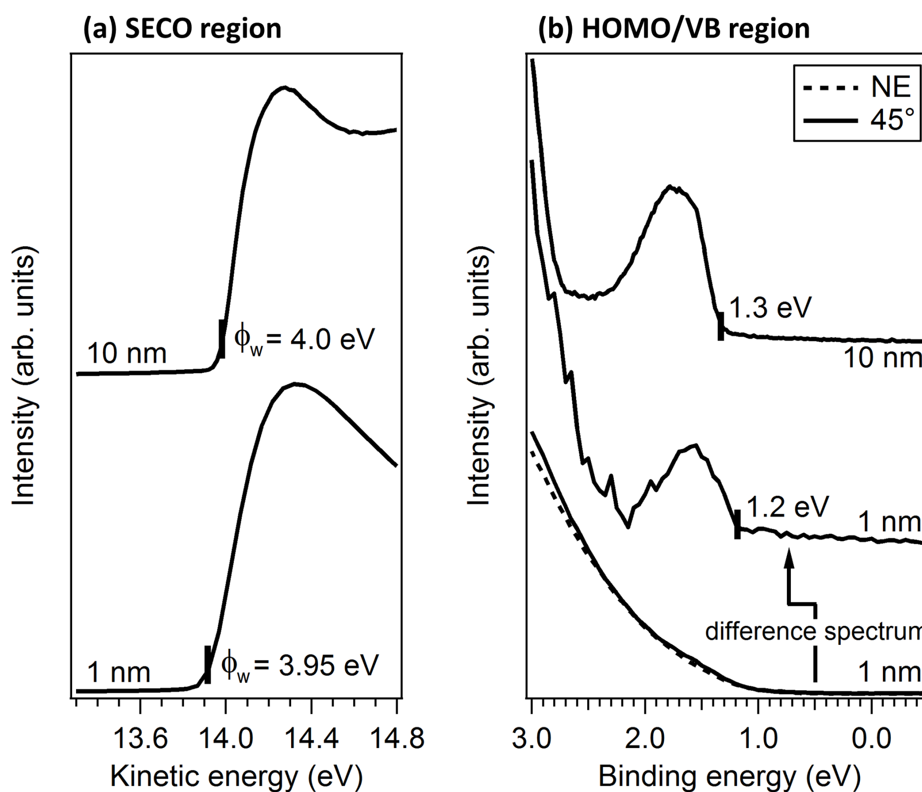

Figure 1: Key results of a UPS measurement of Tc/c-Si interfaces, where the Tc layers were grown ex-situ and transferred to a conventional lab-based UPS apparatus.

2 Derivation of the upper pinhole density and calculation of R_s and R_p values

To conduct the maximum pinhole density measurements we used Tc on c-Si samples that were prepared identically to the devices, except with PEDOT:PSS and the electron contact excluded. AFM micrographs were collected and cross-sections were analysed, searching for voids with flat bases at a consistent depth, consistent with a silicon substrate. Micrographs are shown in Fig. 2. No voids were evident in the 100 nm Tc layer, while the 10 nm Tc layer showed 40% surface coverage by large Tc islands. Using X-ray photoelectron spectroscopy we measured Si 2p signals for the two films, exploiting the high surface sensitivity of XPS to attempt to pick out exposed Si substrate. A large Si 2p signal for the 10 nm film confirmed that silicon was situated at least within a few dye monolayers of empty volume. Note that using this method we were not able to determine if a thin Tc wetting layer existed uniformly over the c-Si surface. No Si XPS signal for the 100 nm sample suggested a closed film in the area probed (approximately 9 mm^2). We arrived at the estimated upper pinhole density of 0.1% in the thick Tc sample by calculating the fraction of deep valleys in the AFM micrograph with base heights of less than 20 nm. This value is consistent with a conservative estimate of S:N in the thin Tc XPS spectrum.

Table 1: Fitting parameters for the intercept models, used to calculate series and shunt resistance

	x-int (V)	y-int (A)	x-int slope	y-int slope	$R_s \Omega/cm^2$	$R_p \Omega/cm^2$
reference	0.644	-0.0223	0.334	0.241E-3	2.99	4.15E3
thin Tc (10 nm)	0.648	-0.0219	0.269	0.207E-3	3.71	4.83E3
thick Tc (100 nm)	0.641	-0.0221	0.562	0.231E-3	1.78	4.34E3

In order to determine the series and shunt resistances of the measured devices, a straight line was fitted to measured points in the vicinity of V_{oc} and I_{sc} for each of the three reported devices. The fits are shown in Figure 3 and the fitting parameters are in Table 1. Series (R_s) and shunt (R_p) resistances were calculated using the following equations:

$$R_s = \left(\frac{\partial I}{\partial V}\right)^{-1} \tag{1}$$

$$R_p + R_s = \left(\frac{\partial I}{\partial V}\right)^{-1} \tag{2}$$

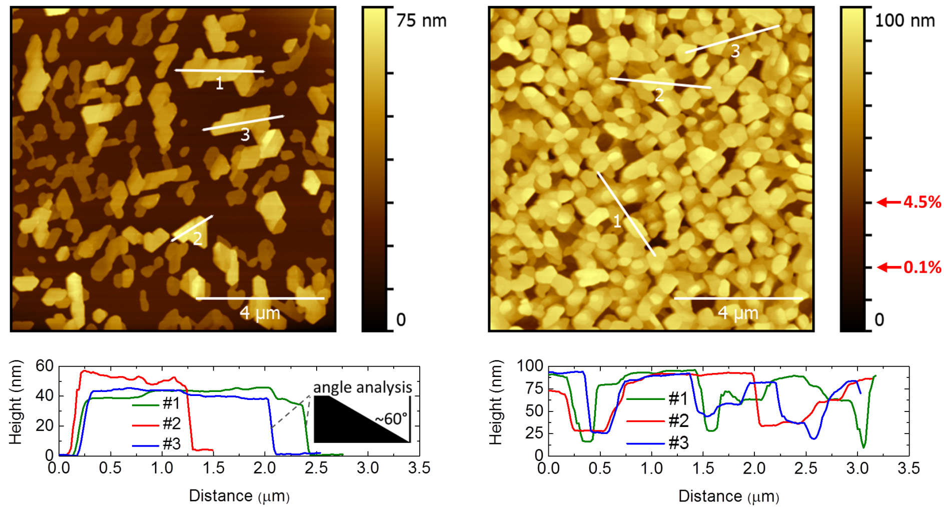

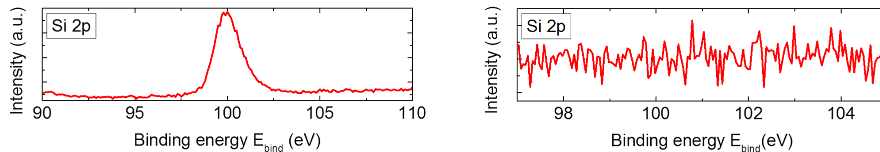

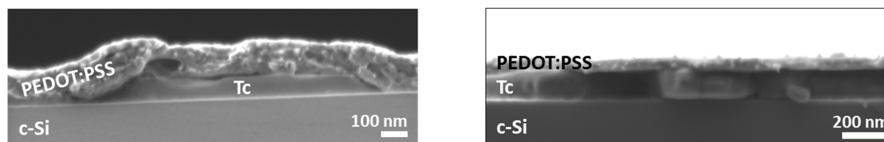

Figure 2: AFM, XPS and SEM data used in the determination of pinhole density of 10 nm and 100 nm Tc films on c-Si. (a) AFM micrographs and cross-sections. (b) X-ray photoelectron spectroscopy Si 2p signal obtained using a commercial XPS source at near-normal incidence. Silicon signal is clearly observed for the 10 nm layer, and not for the 100 nm layer. (c) Scanning electron microscope cross-sections of films with PEDOT:PSS layers added. The morphology of the PEDOT:PSS layer in the thinner Tc sample suggests electrical contact may occur with the c-Si. We have been unable to rule out the presence of a one or two Tc monolayers, which may yet block contact between the c-Si and PEDOT:PSS. In the 100 nm sample, the two materials are clearly separated by the Tc film.

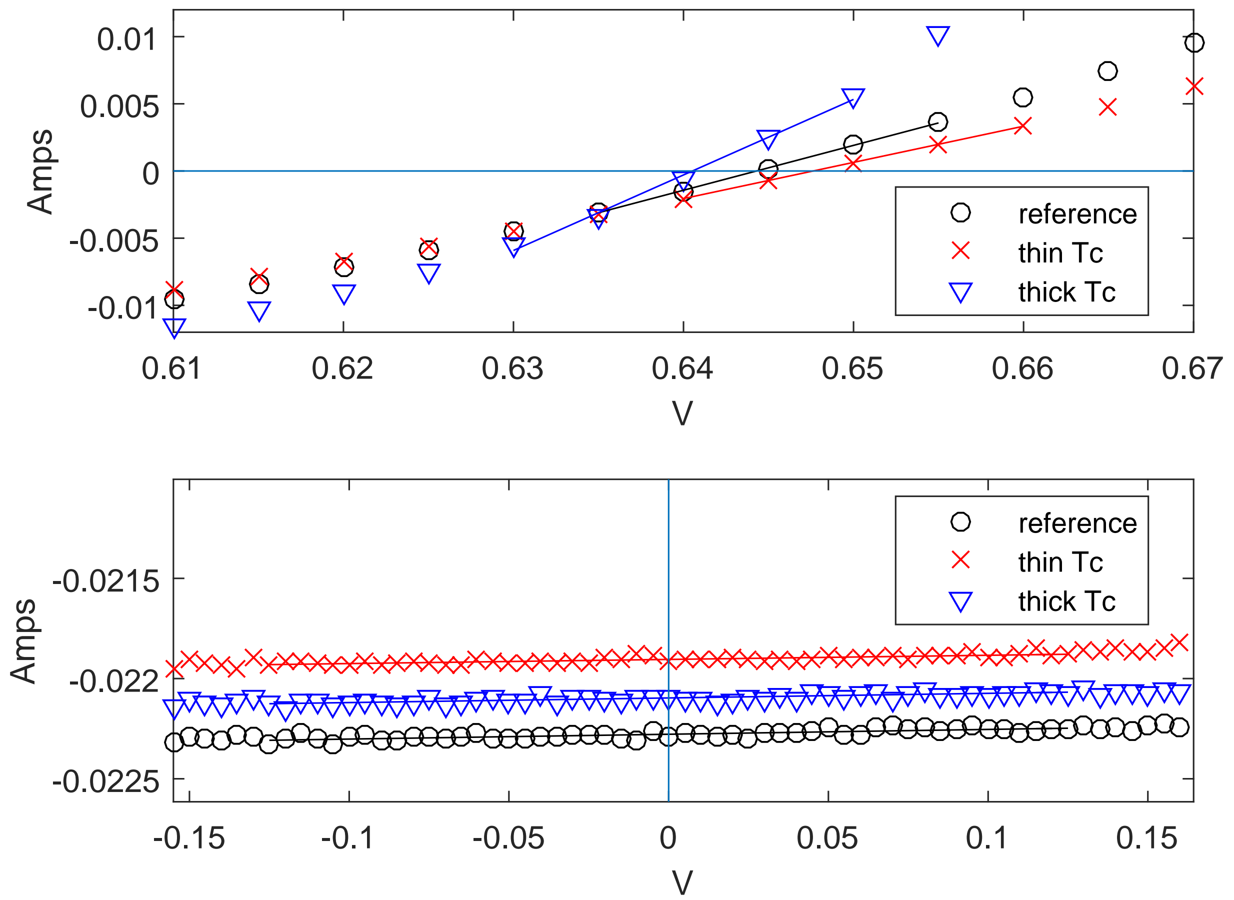

Figure 3: Intercept models for the V_{oc} (top) and I_{sc} (bottom) regions of the measured IV curves. Solid lines indicate fits to the data.

3 Auxiliary EQE measurements: under external bias, and elevated temperatures

The collected spectra are shown in Fig. 4.

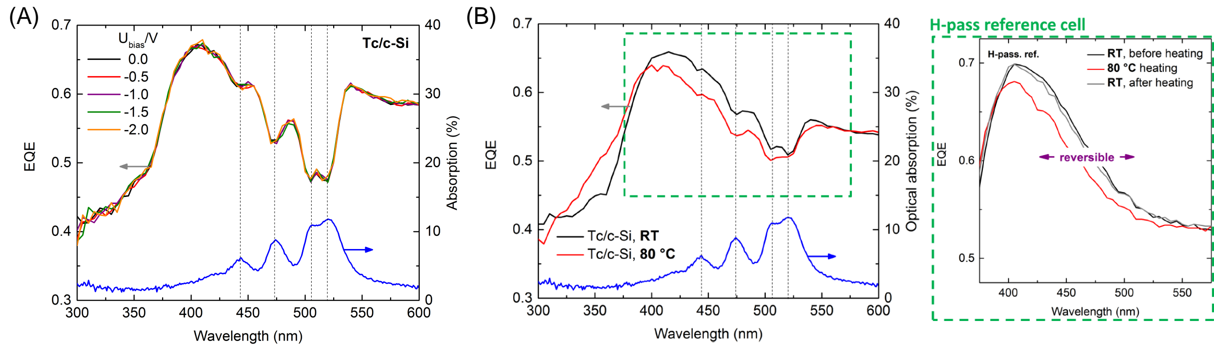

Figure 4: Auxiliary EQE measurements conducted to test possible barriers to triplet exciton harvesting. In (a), the EQE of a 100 nm Tc device does not alter with the indicated applied biases. A Tc absorption spectrum is shown for reference. (b) EQE spectrum of another such cell measured at room temperature and elevated temperatures. While the EQE does alter appreciably, the same behaviour is found for a reference cell that lacks a Tc film and thus cannot be attributed to photocurrent from the organic layer.

4 Device surface coverage by top contact grid

A photograph of the shadow mask used during evaporation of the top metal contact grid is shown in Fig. 5. Boxes drawn over the photograph indicate the area of the contact fingers deposited, and the total device area. The surface coverage by the grid fingers taken over the entire active area is 12%. This shading fraction was not compensated for during current-voltage measurements.

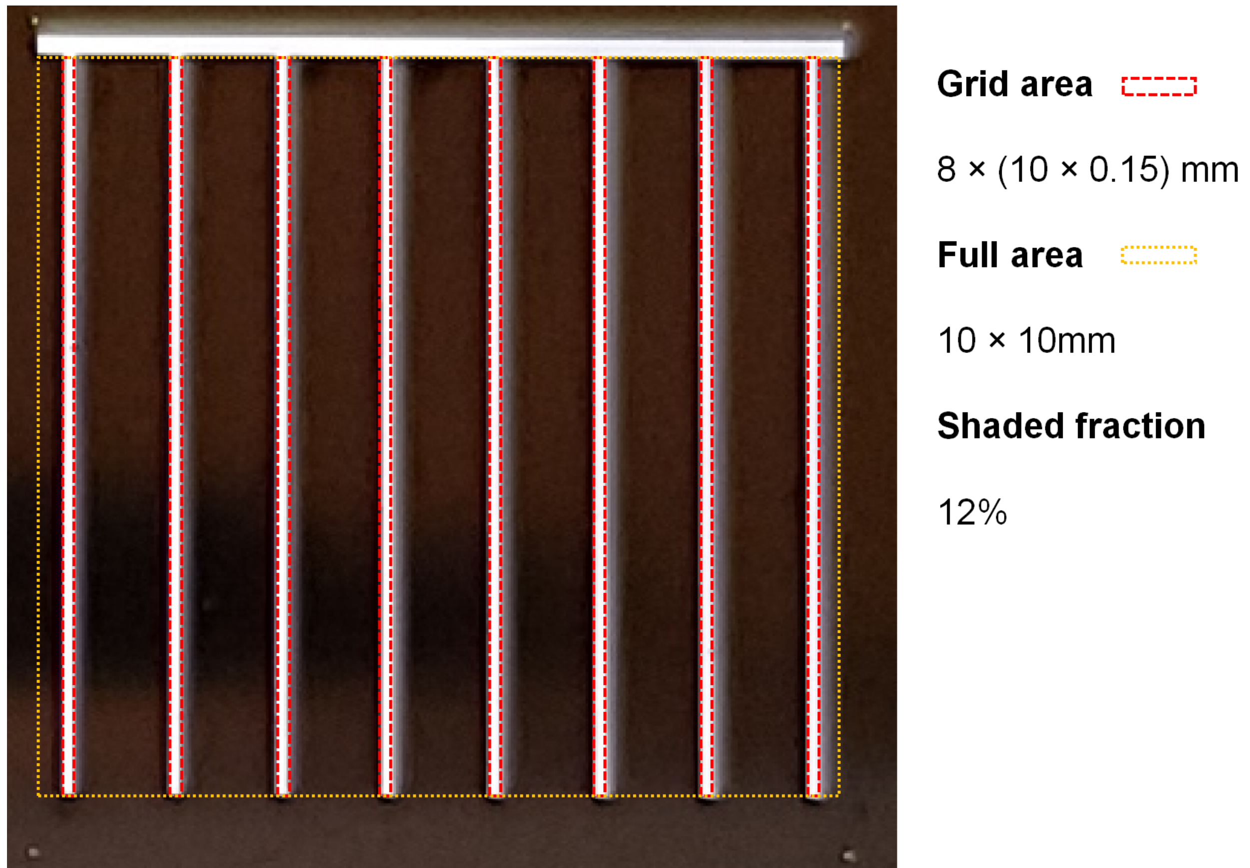

Figure 5: A cropped photograph of a backlit evaporation mask, used during deposition of the metal contact fingers on the top of devices. The fraction of the active area shaded by the contact fingers is indicated.

5 Fitting parameters and spectra from simulations of the external quantum efficiency spectra

Varying f_o, the PEDOT:PSS birefringence parameter, affects the EQE spectrum of the 100 nm Tc device as shown in Fig. 7. Fitting parameters for the GenPro4 simulation of optical structures are presented in Table 2.

Table 2: Optimised fitting parameters obtained for the simulated EQE spectrum of the 100 nm Tc and control devices. η_{Si} and η_{Tc} are the internal quantum efficiencies of current generation in the silicon and tetracene layers, respectively. f_o is the PEDOT:PSS birefringence parameter.

Device	Tc thickness	PEDOT:PSS thickness	η_{Si}	η_{Tc}	f_o
100 nm Tc	120 nm	200 nm	0.99	0.08	0.62
control	–	190 nm	0.99	–	0.85

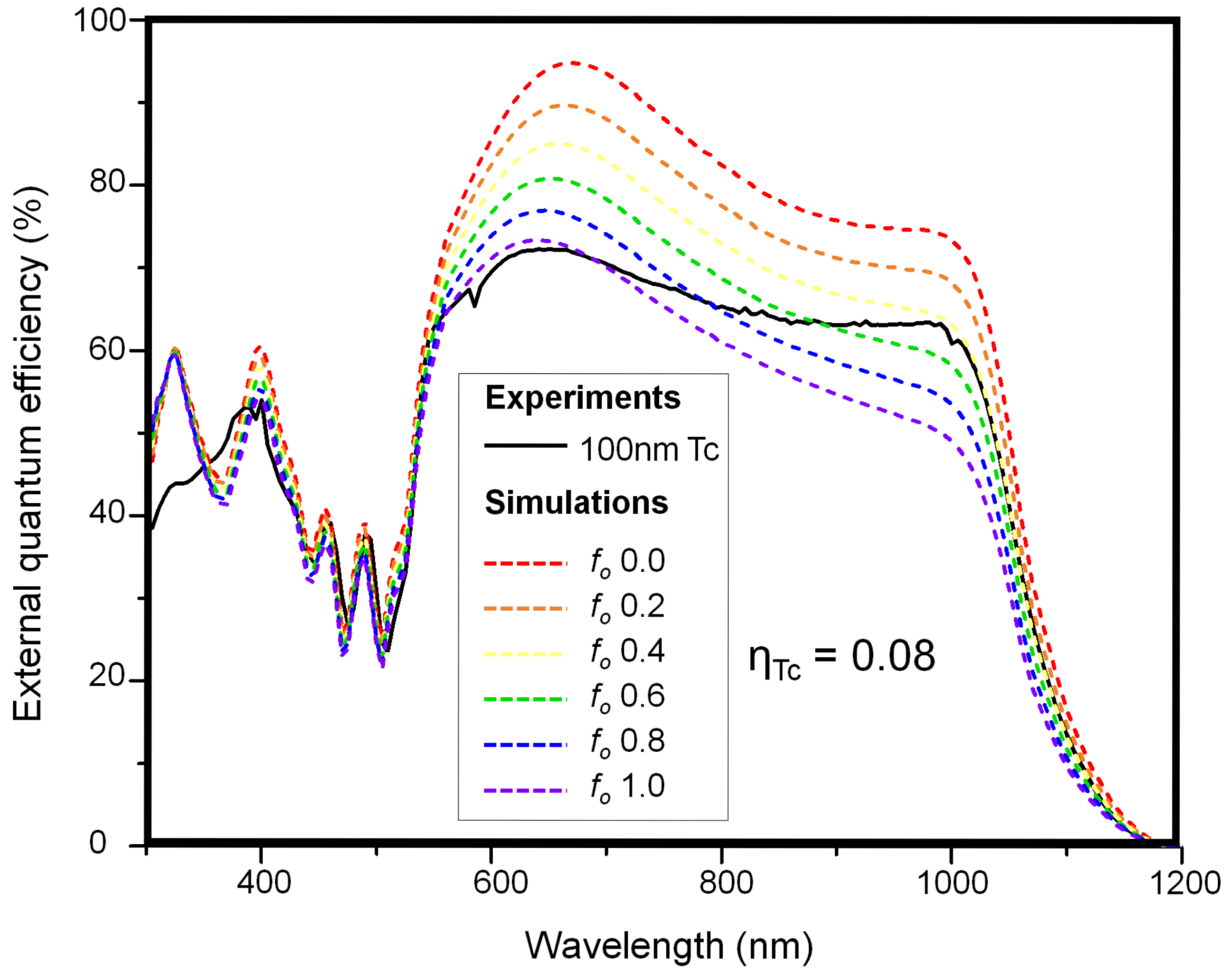

Figure 6: Simulated EQE spectra, alongside the measured spectra of the 100 nm Tc device, demonstrating the effect of changing f_o, the proportion of ordinary/extraordinary optical axis presented to the incident radiation for the PEDOT:PSS overlayer. The portion of the EQE spectrum in the vicinity of the Tc absorption is only weakly affected by this parameter.

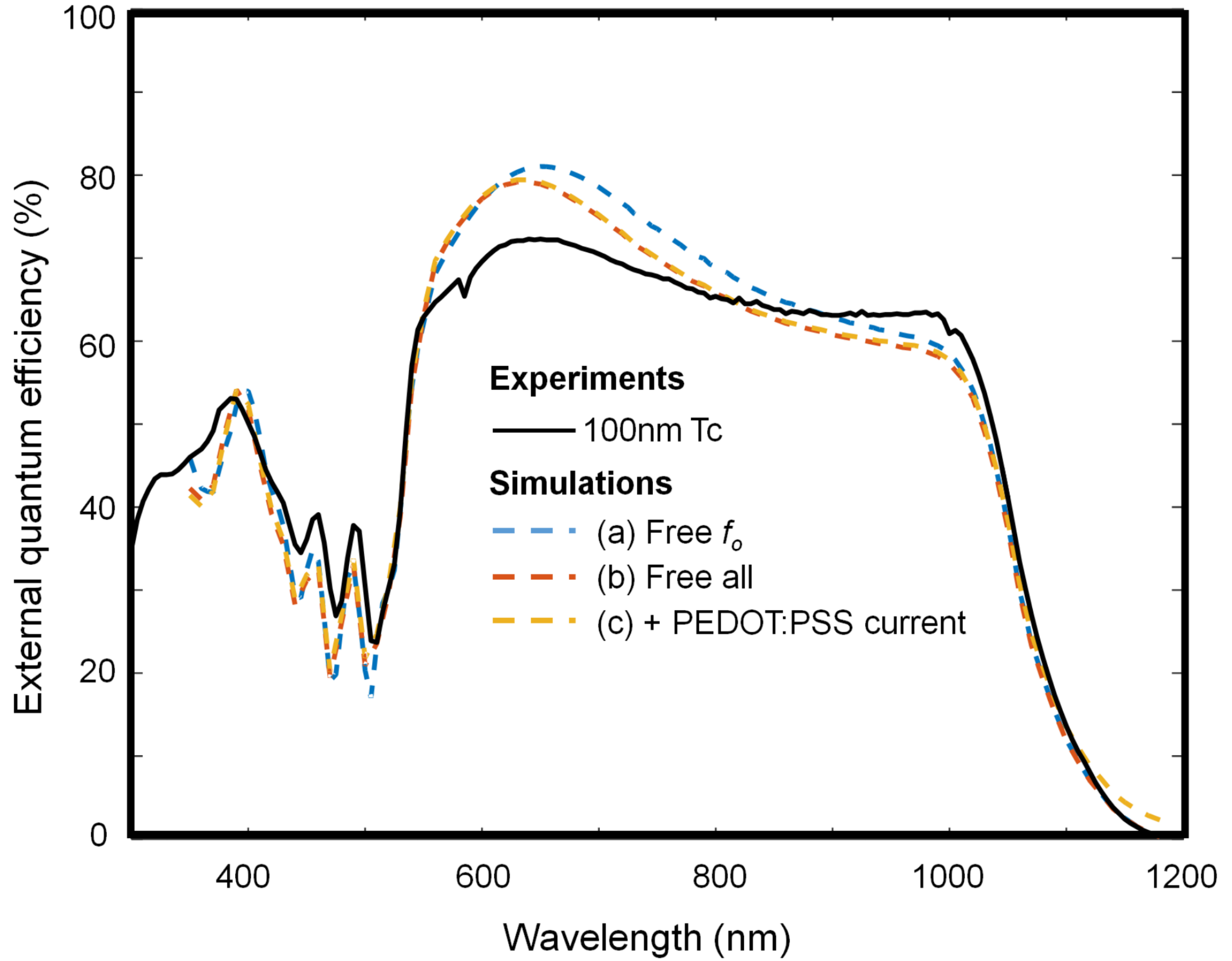

Figure 7: Simulated EQE spectra, alongside the measured spectra of the 100 nm Tc device, demonstrating attempts to fit the measured spectrum while constraining η_{Tc} to zero: (a) using device parameters from Table 2, allowing f_o to vary freely; (b) allowing all layer thicknesses, f_o, and η_{Si} to vary freely; (c) in addition to the conditions in (b), allowing photocurrent generation from the PEDOT:PSS layer with a freely varying internal quantum efficiency. None of the three simulations can reproduce the Tc absorption imprint of the measured device, suggesting a non-zero η_{Tc} value is necessary to correctly model the device.

6 Optical simulations of devices with textured silicon front surface

Modifying the structure of the c-Si Tc heterojunction by texturing the c-Si front surface can greatly reduce the reflectivity of the organo-silicon interface, as shown by simulation in Fig. 8.

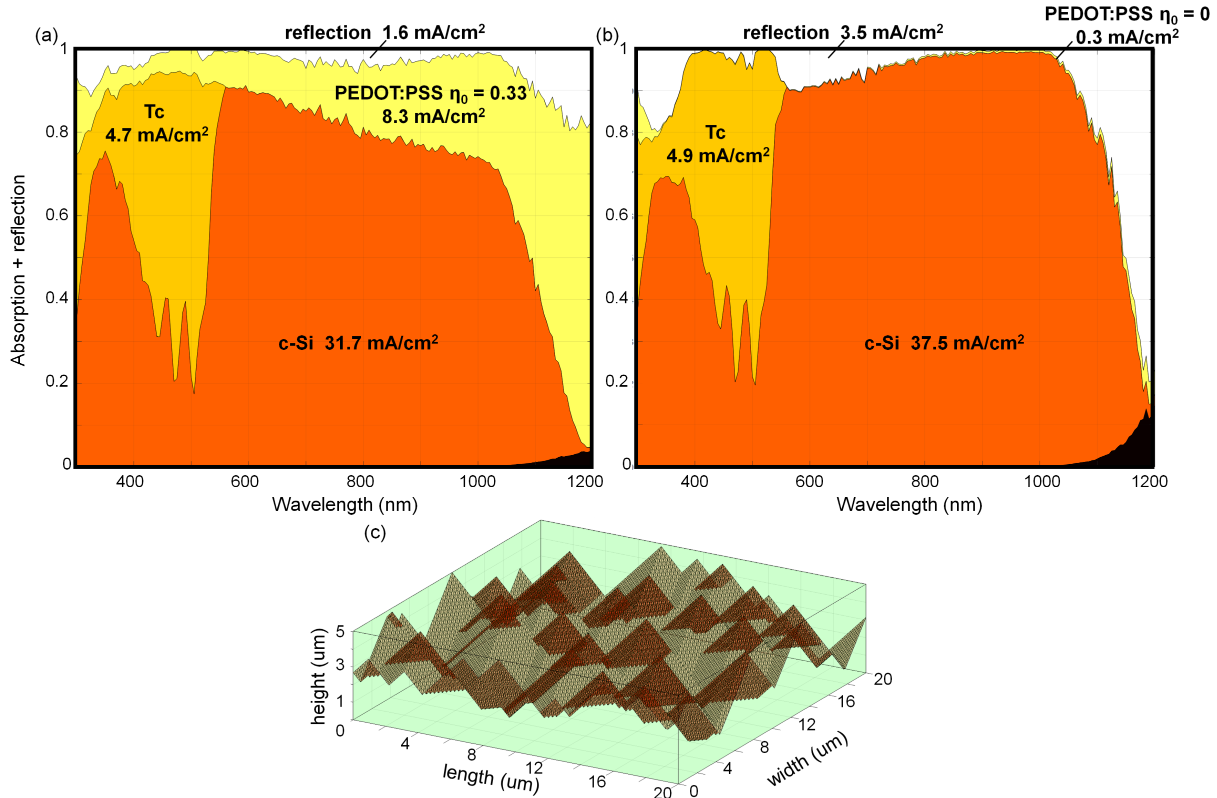

Figure 8: GenPro4 simulations of 100 nm Tc devices utilising a textured silicon surface, which improves light trapping. In (a), the exact device structure of the 100 nm Tc cell is implemented. In (b), the parameter f_o is tuned to reduce parasitic absorption by the PEDOT:PSS layer; the device structure is otherwise unaltered. The reference c-Si textured surface, used in the simulation, is shown in (c).